Journal of Sensor Science and Technology
Vol. 30, No. 6 (2021) pp. 357-363
http://dx.doi.org/10.46670/JSST.2021.30.6.357
pISSN 1225-5475/eISSN 2093-7563

Selective acetate detection using functional carbon nanotube fiber

Seung-Ho Choi[1], Joon-Seok Lee[1], Won-Jun Choi[1], Sungju Lee[2], Hyeon Su Jeong[2], and Seon-Jin Choi[1,+]

Abstract

We developed a chemiresistive anion sensor using highly conductive carbon nanotube fibers (CNTFs) functionalized with anion receptors. Mechanically robust CNTFs were prepared via wet-spinning utilizing the nematic liquid crystal properties of CNTs in chlorosulfonic acid (CSA). For anion detection, polymeric receptors composed of dual-hydrogen bond donors, including thiourea **1**, squaramide **2**, and croconamide **3**, were prepared and bonded non-covalently on the surface of the CNTFs. The binding affinities of the anion receptors were studied using UV–vis titrations. The results revealed that squaramide **2** exhibited the highest binding affinity toward AcO^-, followed by thiourea **1** and croconamide **3**. This trend was consistent with the chemiresistive sensing responses toward AcO^- using functional CNTFs. Selective anion sensing properties were observed that CNTFs functionalized with squaramide **2** exhibited a response of 1.08% toward 33.33 mM AcO^-, while negligible responses (<0.1%) were observed for other anions such as Cl^-, Br^-, and NO_3^-. The improved response was attributed to the internal charge transfer of dual-hydrogen bond donors owing to the deprotonation of the receptor upon the addition of AcO^-.

Keywords : Dual-hydrogen bond donor, Carbon nanotube fiber, Acetate, Chemiresistive anion sensor.

1. INTRODUCTION

The importance of anion detection and sensing is increasing in various fields such as healthcare, environmental monitoring, and biotechnology [1-4]. It has been found that, an excess concentration of acetate anion (AcO^-) inhibits the growth of bacterial cells leading to a low yield of recombinant proteins (e.g., human insulin) [5,6]. Thus, the detection of acetate anion is critical issue in the biotechnology industry to maximize the productivity of recombinant proteins.

Molecules composed of dual-hydrogen bond donors have been demonstrated to be efficient anion binding receptors that utilize hydrogen bond interactions with anions [7]. Various dual-hydrogen bond donors such as urea, thiourea, squaramide, and croconamide have gained considerable attention owing to their versatile utility in the development of anion receptors [8-11]. Novel receptor molecules have been proposed to enhance anion binding affinity by introducing cationic moieties and electron-withdrawing groups combined with dual-hydrogen bond donors, leading to an increase in the acidity of the receptors [12-14]. Furthermore, basic anions such as F^- and AcO^- can effectively interact with the acidic –NH protons of dual-hydrogen bond donor receptors, thereby inducing deprotonation [15].

Various transduction techniques are employed to transduce chemical interactions between receptors and anions into distinguishable signals such as colorimetric, fluorescence, electrochemical, and chemiresistive methods [16,17]. Among these techniques, the chemiresistive method is advantageous for real-time detection owing to its a rapid screening of anionic species. Carbon nanotubes (CNTs) are widely used as electrical signal transducers in chemical sensors [18]. However, the use of pristine CNTs for the development of chemical sensors is limited owing to the low chemical reactivity and large signal noise generated by poor adhesion to the sensor substrate [19,20].

To overcome these limitations, we adopted carbon nanotube fibers (CNTFs) which have high electrical conductivity and mechanical strength. CNTFs composed of axially aligned CNTs exhibited high electrical conductivity owing to the π conjugation of the CNT sidewalls. To further enhance the anion-binding capability of CNTFs, the functionalization of receptors was essential inducing chemical interactions, that could be transduced into electrical signals through the CNTFs. Receptors can be

[1] Division of Materials Science and Engineering, Hanyang University, 222 Wangsimni-ro, Seongdong-gu, Seoul 04763, Republic of Korea
[2] Institute of Advanced Composite Materials, Korea Institute of Science and Technology (KIST) 92 Chudong-ro, Bongdong-eup, Wanju-gun, Jeonrabuk-do 565-905, Republic of Korea
[+] Corresponding author: sjchoi27@hanyang.ac.kr
(Received: Oct. 15, 2021, Accepted : Nov. 19, 2021)

functionalized on the surface of CNTFs by either covalent or non-covalent bonding [21]. For covalent bonding, receptors penetrate through C=C bonds and disrupt π conjugation leading to a decrease in conductivity [22]. On the other hand, non-covalent functionalization can preserve the π conjugation of the CNT sidewall, thus maintaining high electrical conductivity. Non-covalent functionalization can be achieved by physically wrapping the CNTFs using polymers such as poly(4-vinyl pyridine) (P4VP) [23].

Herein, we report functional CNTF composites that facilitate the non-covalent functionalization of dual-hydrogen bond donor-based receptors for the detection of anions. Various receptor molecules composed of thiourea **1**, squaramide **2**, and croconamide **3** were synthesized, and their anion binding affinities were evaluated. The chemiresistive sensing properties were investigated upon the injection of analytes, which can be applied in real-time anion detection with small samples.

2. EXPERIMENTAL

2.1 Materials

All chemicals and reagents were purchased from Sigma-Aldrich and were used without additional purification. 3-bromopropylamine hydrobromide, triethylamine, 6-amino-1-hexanol, and iodomethane were purchased from Sigma-Aldrich. 3,5-bis(trifluoromethyl) phenyl isothiocyanate, 3,4-dimethoxycyclobut-3-ene-1,2-dione, and 3,5-bis(trifluoromethyl)aniline were purchased from TCI Chemical. Croconic acid, $AgNO_3$, and hydrobromic acid (48% aqueous) were purchased from Alfa Aesar. Poly(4-vinyl pyridine) (M_w = 200,000) was purchased from Scientific Polymer Product, Inc. Single-walled carbon nanotubes (CNTs) were purchased from OCSiAl.

2.2 Synthesis of CNTFs

The CNTFs were synthesized via wet-spinning (Fig. 1(a)). First, single-walled carbon nanotubes (SWCNTs) powders were purified and dispersed in chlorosulfonic acid (CSA) at a concentration of 4 wt%. Then, the continuous fiber was obtained by the coagulation of the SWCNT dispersion in acetone through the wet-spinning technique. The obtained fibers were dried in a vacuum oven at 80 °C.

2.3 Synthesis of Thiourea 1-P4VP

To synthesize thiourea-functionalized P4VP (thiourea **1**-P4VP), P4VP-3-bromopropylamine hydrobromide was first prepared via the reaction between P4VP (100 mg, 1.26 mmol) and 3-bromopropylamine hydrobromide (400 mg, 1.82 mmol) in dimethylformamide (DMF) at 60 °C for 3 days. Subsequently, **1**-P4VP was obtained via the reaction between P4VP-3-bromopropylamine hydrobromide (57 mg, 0.19 mmol), 3,5-bis(trifluoromethyl)phenyl isothiocyanate (41 μL, 0.38 mmol) and triethylamine (80 μL, 0.57 mmol) in 30 mL of methanol (MeOH) at room temperature for 3 days.

2.4 Synthesis of Squaramide 2-P4VP

For the synthesis of squaramide-functionalized P4VP (**2**-P4VP), 3-((3,5-bis(trifluoromethyl)phenyl)amino)-4-methoxycyclobut-3-ene-1,2-dione was prepared by dissolving 3,4-dimethoxycyclobut-3-ene-1,2-dione (500 mg, 3.5205 mmol) in MeOH (20 mL) and stirred with 3,5-bis(trifluoromethyl)aniline (522 μL, 3.444 mmol). The mixture was refluxed for 3 days. The solution was concentrated in vacuum, redispersed in water, and filtered to obtain 3-((3,5-bis(trifluoromethyl)phenyl)amino)-4-methoxycyclobut-3-ene-1,2-dione. This product (200 mg, 0.59 mmol) was then stirred with 3-bromopropylamine hydrobromide (200 mg, 0.7079 mmol) and triethylamine (99 μL, 0.7079 mmol) in MeOH (10 mL) at 60 °C for 3 days. The solution was concentrated in vacuum and washed with water to obtain the required product (i.e., 3-((3,5-bis(trifluoromethyl)phenyl)amino)-4-((3-bromopropyl)amino) cyclobut-3-ene-1, 2-dione).

To synthesize squaramide **2**-P4VP, P4VP (38 mg) was dissolved in DMF (10 mL) with 3-((3,5-bis(trifluoromethyl)phenyl)amino)-4-((3-bromopropyl)amino)cyclobut-3-ene-1,2-dione (200 mg, 0.4528 mmol) and stirred for 3 days at 85 °C. After cooling, the mixture was concentrated with vacuum and redispersed in acetonitrile (CH_3CN) to obtain squaramide **2**-P4VP.

2.5 Synthesis of Croconamide 3-P4VP

For the synthesis of disilver croconate, $AgNO_3$ (1.196 g, 7.04 mmol) was added to the solution of croconic acid (400 mg, 2.82 mmol) and dissolved in water (20 mL). The mixture was stirred in the dark for 1 h at room temperature. Disilver coconate was obtained by filtering and washing the resulting precipitate.

Disilver croconate was dissolved in 15 mL of dry toluene and

then iodomethane (385 μL, 6.18 mmol) was added. The mixture was stirred and refluxed for 5 h. The solution was concentrated under vacuum and redispersed in diethyl ether to obtain dimethyl croconate.

6-amino-1-hexanol (650 mg, 5.55 mmol) was added to 5 mL of 48% aqueous hydrobromic acid (HBr) and the solution was refluxed for 6 h. The solution was concentrated under vacuum and dried for 1 day at 60 °C. 6-bromohexan-1-amine hydrobromide was obtained as the product after washing and filtering with ethyl acetate.

Dimethyl croconate was mixed with 3,5-bis(trifluoro methyl)aniline (39 μL, 0.24 mmol) in 5 mL of MeOH. The mixture was stirred and refluxed for 1 day. 6-bromohexan-1-amine hydrobromide (60.92 mg, 0.24 mmol) and trimethylamine (49.25 μL, 0.35 mmol) were added and refluxed for 1 day. The required product, i.e., 4-((3,5-bis(trifluoromethyl) phenyl)amino)-5-((6-bromohexyl) amino)cyclopent-4-ene 1, 2,3-trione was obtained by column chromatography (DCM:MeOH=98%:2%).

P4VP (10.92 mg, 0.1381 mmol) was dissolved in 1 mL of DMF, and then 5 mL of CH_3CN was added. 4-((3,5-bis(trifluoromethyl) phenyl)amino)-5-((6-bromohexyl)amino)cyclopent-4-ene1,2,3-trione (71 mg, 0.1381 mmol) was added to the solution. The reaction mixture was stirred and refluxed at 90 °C. The solution was concentrated under vacuum and redispersed in CH_3CN. The product was washed and filtered with CH_3CN to obtain croconamide **3**-P4VP.

2.6 Receptor Functionalization on CNTF Surface

Receptors composed of dual-hydrogen bond donors were functionalized on the surface of the CNTFs by the dip-coating method. The dip-coating solution was prepared by dissolving receptors (i.e., **1**-P4VP, **2**-P4VP, and **3**-P4VP) in MeOH at a concentration of 1 mg mL^{-1}. Subsequently, the CNTFs were immersed in each solution for 1 h and dried in air.

2.7 Sensor Fabrication

To fabricate the anion sensor, functionalized CNTFs were welded with silver paste to attach them to a glass substrate and form electrical contacts. Then, a polydimethylsiloxane mold with a cylindrical chamber having a diameter of 3 mm was attached to the top of the glass substrate to isolate the sensing environment and electrical contacts (Fig. 1(b)). For the sake of comparison, pristine CNTF sensors were prepared as well using similar methods without receptor functionalization.

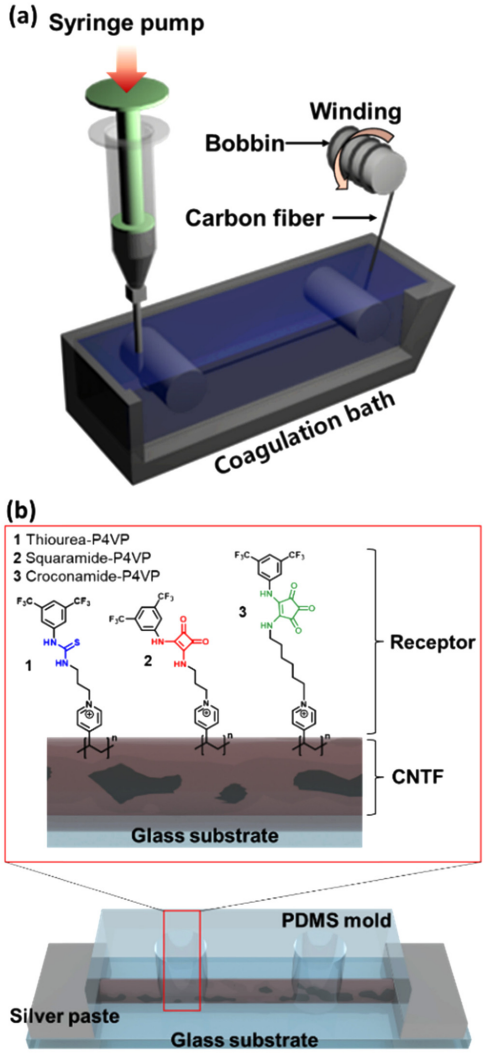

Fig. 1. Schematic illustrations of (a) the wet-spinning technique and (b) CNTF sensor functionalized with dual-hydrogen bond donor- based receptors (thiourea **1**-P4VP, squaramide **2**-P4VP, and croconamide 3-P4VP).

2.8 Anion Sensing Characterization

To investigate the anion-sensing properties of **1**-P4VP-CNTF, **2**-P4VP-CNTF, and **3**-P4VP-CNTF, baseline resistance was stabilized by injecting 10 μL of CH_3CN into the solution chamber. Then, 2 μL of anion solution at a concentration of 5–33.33 mM was additionally injected into the solution chamber and the resistance transition of the sensor was monitored. The anion analyte solutions were prepared by dissolving acetate (AcO^-), nitrate (NO_3^-), bromide (Br^-), and chloride (Cl^-) with a tetrabutylammonium-based salt in CH_3CN. The sensor responses were defined as the normalized resistance change, i.e., $(R_{anion}–R_0)/R_0$ (%), where R_{anion} is the resistance after injection of the analyte

Table 1. Binding constants of the receptors calculated based on UV–vis titrations.

Binding constant	1	2	3
$K_{11}[M^{-1}]$	3.44×10^5	7.34×10^5	3.21×10^5
$K_{12}[M^{-1}]$	2.84×10^4	1.50×10^6	-

solution and R_0 is the baseline resistance.

3. RESULTS AND DISCUSSIONS

The chemiresistive anion sensor was developed to transduce the chemical interactions between the anions and receptors into electrical signals. CNTFs, which were synthesized by the wet-spinning technique, were used as electrical transducers (Fig. 1(a)). Three different types of receptors (e.g., thiourea **1**, squaramide **2**, and croconamide **3**) were non-covalently functionalized on the surface of the CNTFs to compare the anion-sensing properties (Fig. 1(b)).

To study the anion-binding properties, the model structures of the receptors were synthesized by replacing P4VP with pyridine. UV–vis titrations were performed using model receptors for AcO^-, NO_3^-, Br^-, and Cl^- in dimethyl sulfoxide (DMSO) or dichloromethane (DCM). The results revealed that the absorbance intensity around 330 nm of receptor **1** increased after the addition of AcO^- in DMSO (Fig. 2(a)). The enhanced absorbance is attributed to the binding of **1** and AcO^-. The 1:2 binding stoichiometry of receptor **1** toward AcO^- implies the deprotonation of receptor **1**, producing a hydrogen-bonding self-complex AcO^- ($[H^+(AcO)_2]^-$) [24]. Similarly, receptor **2** exhibited enhanced absorbance intensity around 390 nm after the addition of AcO^- in DMSO. Additionally, a decrease in intensity was observed around 280 nm, 320 nm, and 350 nm (Fig. 2(b)). The absorbance changes were attributed to the formation of the **2**-AcO^- complex. An increased concentration of AcO^- induced the deprotonation of receptor **2**, leading to a 1:2 binding stoichiometry and formation of the hydrogen-bond self-complex AcO^-. Furthermore, receptor **3** exhibited increased absorbance intensity around 420 nm with the disappearance of the absorbance peak at 372 nm upon the addition of AcO^- in DCM (Fig. 2(c)). The absorbance changes were explained by the deprotonation of receptor **3** with the addition of AcO^-. A binding stoichiometry of 1:1 was observed for receptor **3** toward AcO^-, which was mainly attributed to the initial deprotonation of receptor **3** in DCM due to strong acidity [25].

Absolute absorbance changes (ΔAbs) were calculated using characteristic absorbance peaks from UV–vis titrations (Fig. 2(d)–(f)). All receptors showed the highest absorbance changes toward AcO^-, with negligible changes toward NO_3^-, Br^-, and Cl^-. The binding constants (K_{11}) of receptors **1**, **2**, and **3** implied strong interactions with AcO^- in the order of **2** > **1** > **3** (Table 1).

CNTFs were synthesized via wet-spinning, facilitating the nematic liquid crystal (LC) behavior of the SWCNT dispersion in CSA. Birefringence with the schlieren texture was observed from

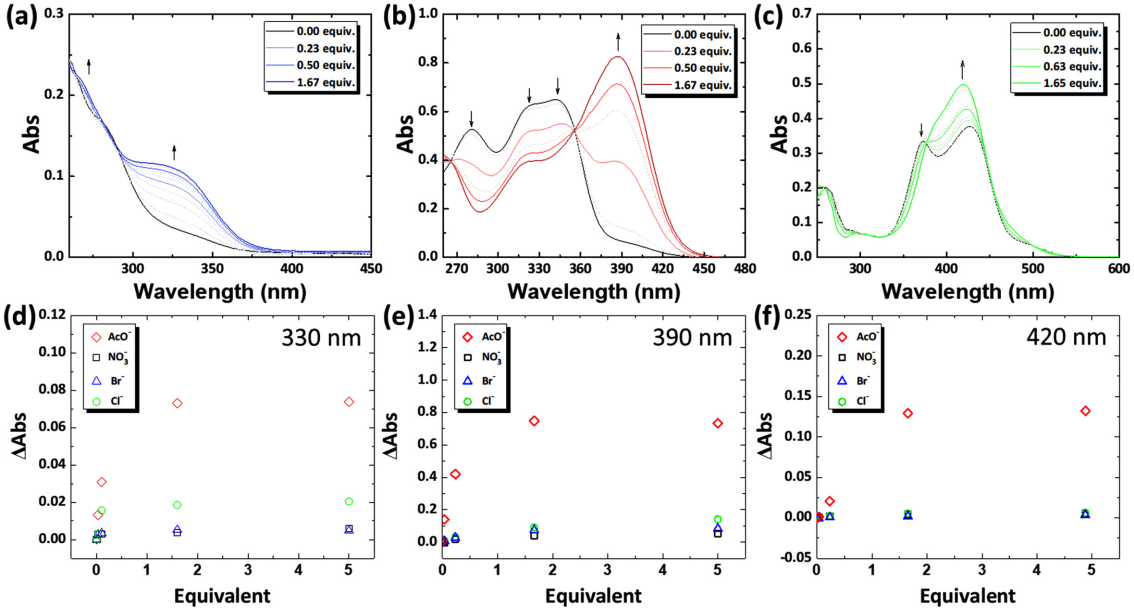

Fig. 2. UV–vis titrations of (a) thiourea **1**, (b) squaramide **2**, and (c) croconamide **3** upon addition of AcO^-. Absolute absorbance (ΔAbs) changes of (d) thiourea **1**, (e) squaramide **2**, and (f) croconamide **3** toward AcO^-, NO_3^-, Br^-, and Cl^-.

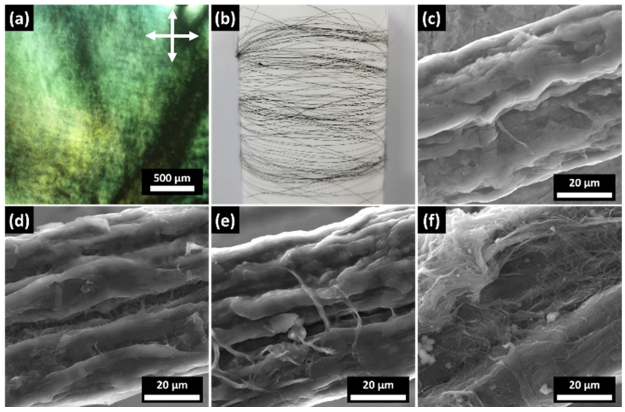

Fig. 3. (a) Polarized optical microscopy (POM) image of CNT LCs in CSA. (b) Camera image of as-spun CNTF. Scanning electron microscopy (SEM) images of (c) pristine CNTF, (d) **1**-P4VP-CNTF, (e) **2**-P4VP-CNTF, and (f) **3**-P4VP-CNTF.

the SWCNT dispersion using polarized optical microscopy (POM) (Fig. 3(a)). The aligned CNTs in the polarizer direction can be confirmed from the dark region in the POM image. CNTFs were easily collected on a bobbin and the continuous fiber structure was obtained owing to the coagulation of CNTs during the wet-spinning process (Fig. 3(b)). From the SEM images, CNTF showed a one-dimensional structure and rough surface morphology with a diameter of approximately 53 μm (Fig. 3(c)). For non-covalently functionalized CNTFs, polymeric receptors were physically attached exhibiting polymeric chains on the surface of the CNTFs (Fig. 3(d)–(f)). **1**-P4VP-CNTFs and **2**-P4VP-CNTFs presented homogenous surface coatings with **1**-P4VP and **2**-P4VP, respectively, mainly owing to the high solubility of the receptors in the dip-coating solution (i.e., MeOH). In contrast, **3**-P4VP had low solubility in the dip-coating solution, which resulted in partial agglomeration on the surface of the CNTFs.

The anion-sensing characteristics of the CNTF sensors were evaluated upon the addition of AcO^-, NO_3^-, Br^-, and Cl^- (Fig. 4). The real-time response changes of anion sensors were observed toward anions in the concentration range of 5–33.33 mM. Before the injection of the analyte solution, pure CH_3CN (10 μL) was injected into the sensing chamber to stabilize the baseline resistance, resulting in decreased resistance. After stabilization for approximately 5 min, an anion solution (2 μL) was injected to measure the sensor resistance transitions.

First, the sensing properties of the pristine CNTFs were evaluated. Pristine CNTFs showed negligible response toward 33.33 mM of AcO^-. After functionalization of dual-hydrogen bond donor-based receptors, the resistance of the functional CNTFs increased upon the addition of the analyte anion solution. The results revealed that the resistance of **1**-P4VP-CNTF increased with increasing AcO^- concentration exhibiting a response of 0.82% at 33.33 mM AcO^- (Fig 4(a)). The experimental detection limit for **1**-P4VP-CNTF was 5 mM, with a response of 0.20%. For **2**-P4VP-CNTF, improved AcO^- sensing properties were achieved with a response of 1.08% and 0.26% at 33.33 mM and 5 mM of AcO^-, respectively (Fig 4(b)). In the case of **3**-P4VP-CNTF, the anion sensor showed a response of 0.44% and 0.05% at 33.33 mM and 5 mM of AcO^- (Fig 4(c)). The highest sensing response was observed with the **2**-P4VP-CNTFs, which was in good agreement with the results of the UV–vis titrations and calculated binding constants of the receptor molecules. The improved AcO^- sensing response for **2**-P4VP-CNTFs can be explained by the efficient deprotonation of the squaramide groups upon the injection of basic anions, resulting in large resistance changes. After deprotonation of the receptors, internal charge transfer occurred in the polymeric receptor, causing the modulation of the surface charge density. Specifically, negatively charged receptors trapped holes in the CNTFs after deprotonation, thereby producing increased resistance transitions.

Selective AcO^- sensing properties were evaluated for **2**-P4VP-CNTF; negligible responses (<0.1%) were observed for NO_3^-, Br^-, and Cl^- (Fig 4(d)). Low responses toward interfering anions were mainly attributed to the hydrogen bonding interactions between the receptors and anions (i.e., NO_3^-, Br^-, and Cl^-),

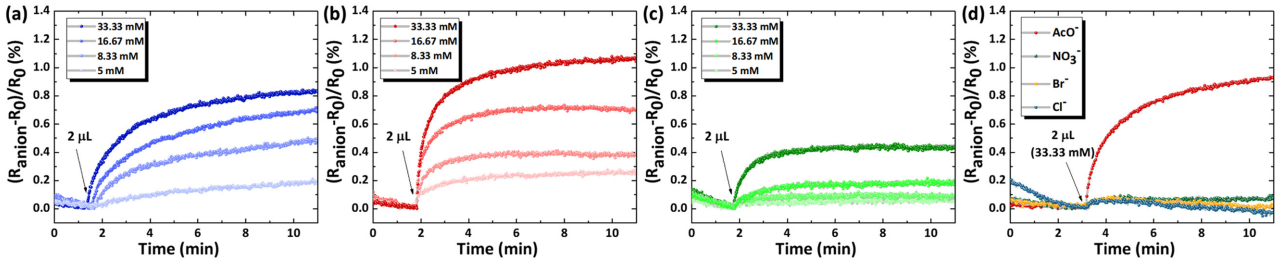

Fig. 4. Dynamic response transitions of (a) **1**-P4VP-CNTF, (b) **2**-P4VP-CNTF, and (c) **3**-P4VP-CNTF upon addition of AcO^- in the concentration range of 5–33.33 mM in acetonitrile (CH_3CN). (d) Sensor responses of **2**-P4VP-CNTF toward 33.33 mM of AcO^-, NO_3^-, Br^-, and Cl^-.

resulting in minor resistance changes in the CNTFs. This result was consistent with the UV–vis titrations, wherein there were minor absolute absorbance changes in the receptors upon the addition of NO_3^-, Br^-, and Cl^-.

4. CONCLUSIONS

In summary, a real-time chemiresistive anion sensor was developed using functional CNTFs for the selective detection of AcO^-. Anion receptors comprising dual-hydrogen bond donors (i.e., thiourea **1**, squaramide **2**, and croconamide **3**) were synthesized by introducing a cationic moiety (pyridinium) and an electron-withdrawing group (3,5-bis(trifluoromethyl)-phenyl). The anion binding properties of the model structures were investigated using UV–vis titrations in DMSO or DCM, wherein the binding affinity toward AcO^- was in the order of **2** > **1** > **3**. To transduce chemical interactions into electrical signals, electrically conductive and mechanically stable CNTFs were prepared via the wet-spinning process. Subsequently, the receptors were non-covalently functionalized on the surface of the CNTFs using the dip-coating method. Chemiresistive anion sensing properties showed that a high response [$(R_{anion}–R_0)/R_0$ (%)] of 1.08% was achieved at a 33.33 mM AcO^- with a **2**-P4VP-CNTF sensor, which was mainly attributed to the efficient deprotonation of the dual-hydrogen bond donors (squaramide) that induced internal charge transfer. In addition, negligible responses (<0.1%) were observed for interfering analytes such as NO_3^-, Br^-, and Cl^- as a result of weak hydrogen bonding interactions with the receptor. The unique chemiresistive anion-sensing platform can be used for point-of-care tests with real-time wireless detection of anions.

ACKNOWLEDGMENT

This study was supported by the National Research Foundation of Korea (NRF) grant funded by the Korean government (MSIT) (No. 2020R1C1C1010336). This study was also supported by the U.S. Army Combat Capabilities Development Command Soldier Center (DEVCOM SC) and International Technology Center Pacific (ITC-PAC) Global Research Project under contract FA520920P0130 and conducted at Hanyang University.

REFERENCES

[1] R. Z. Wu, X. Yang, L. W. Zhang, and P. P. Zhou, “Luminescent lanthanide metal–organic frameworks for chemical sensing and toxic anion detection”, *Dalton Trans.*, Vol. 46, No. 30, pp. 9859-9867, 2017.

[2] M. T. Gabr and F. C. Pigge, “A fluorescent turn-on probe for cyanide anion detection based on an AIE active cobalt (II) complex”, *Dalton Trans.*, Vol. 47, No. 6, pp. 2079-2085, 2018.

[3] Y. Qin, A. U. Alam, S. Pan, M. M. Howlader, R. Ghosh, N.-X. Hu, H. Jin, S. Dong, C. H. Chen, and M. J. Deen, “Integrated water quality monitoring system with pH, free chlorine, and temperature sensors”, *Sens. Actuator B-Chem.*, Vol. 255, No. 1, pp. 781-790, 2018.

[4] J. Xu, Y. Fang, and J. Chen, “Wearable Biosensors for Non-Invasive Sweat Diagnostics”, *Biosensors*, Vol. 11, No. 8, pp. 245(1)-245(21), 2021.

[5] A. J. Wolfe, “The acetate switch”, *Microbiol. Mol. Biol. Rev.*, Vol. 69, No. 1, pp. 12-50, 2005.

[6] S. Pinhal, D. Ropers, J. Geiselmann, and H. de Jong, “Acetate Metabolism and the Inhibition of Bacterial Growth by Acetate”, *J. Bacteriol.*, Vol. 201, No. 13, pp. e00147-19(1)-e00147-19(19), 2019.

[7] L. Chen, S. N. Berry, X. Wu, E. N. Howe, and P. A. Gale, “Advances in anion receptor chemistry”, *Chem*, Vol. 6, No. 1, pp. 61-141, 2020.

[8] Y. Wu, X. Peng, J. Fan, S. Gao, M. Tian, J. Zhao, and S. Sun, “Fluorescence sensing of anions based on inhibition of excited-state intramolecular proton transfer”, *J. Org. Chem.*, Vol. 72, No. 1, pp. 62-70, 2007.

[9] B. Zavala-Contreras, H. Santacruz-Ortega, A. U. Orozco-Valencia, M. Inoue, K. Ochoa Lara, and R.-E. Navarro, “Optical Anion Receptors with Urea/Thiourea Subunits on a TentaGel Support”, *ACS omega*, Vol. 6, No. 14, pp. 9381-9390, 2021.

[10] G. Picci, M. Kubicki, A. Garau, V. Lippolis, R. Mocci, A. Porcheddu, R. Quesada, P. C. Ricci, M. A. Scorciapino, and C. Caltagirone, “Simple squaramide receptors for highly efficient anion binding in aqueous media and transmembrane transport”, *Chem. Commun.*, Vol. 56, No. 75, pp. 11066-11069, 2020.

[11] V. E. Zwicker, K. K. Yuen, D. G. Smith, J. Ho, L. Qin, P. Turner, and K. A. Jolliffe, “Deltamides and Croconamides: Expanding the Range of Dual H-bond Donors for Selective Anion Recognition”, *Chem. Eur. J.*, Vol. 24, No. 5, pp. 1140-1150, 2018.

[12] I. Sandler, F. A. Larik, N. Mallo, J. E. Beves, and J. Ho, “Anion Binding Affinity: Acidity versus Conformational Effects”, *J. Org. Chem.*, Vol. 85, No. 12, pp. 8074-8084, 2020.

[13] G. Bergamaschi, M. Boiocchi, E. Monzani, and V. Amendola, “Pyridinium/urea-based anion receptor: methine formation in the presence of basic anions”, *Org. Biomol.*

Chem., Vol. 9, No. 24, pp. 8276-8283, 2011.
[14] S. J. Choi, B. Yoon, J. D. Ray, A. Netchaev, L. C. Moores, and T. M. Swager, "Chemiresistors for the Real-Time Wireless Detection of Anions", *Adv. Funct. Mater.*, Vol. 30, No. 7, pp. 1907087(1)-1907087(9), 2020.
[15] S. Ha, J. Lee, K.-s. Kim, E. J. Choi, P. Nhem, and C. Song, "Anion-responsive thiourea-based gel actuator", *Chem. Mater.*, Vol. 31, No. 15, pp. 5735-5741, 2019.
[16] R. Hein, P. D. Beer, and J. J. Davis, "Electrochemical anion sensing: supramolecular approaches", *Chem. Rev.*, Vol. 120, No. 3, pp. 1888-1935, 2020.
[17] D. A. McNaughton, M. Fares, G. Picci, P. A. Gale, and C. Caltagirone, "Advances in fluorescent and colorimetric sensors for anionic species", *Coord. Chem. Rev.*, Vol. 427, pp. 213573(1)- 213573(44), 2021.
[18] V. Schroeder, S. Savagatrup, M. He, S. B. Ling, and T. M. Swager, "Carbon Nanotube Chemical Sensors", *Chem. Rev.*, Vol. 119, No. 1, pp. 599-663, 2019.
[19] H. C. Su, C. H. Chen, Y. C. Chen, D. J. Yao, H. Chen, Y. C. Chang, and T. R. Yew, "Improving the adhesion of carbon nanotubes to a substrate using microwave treatment", *Carbon*, Vol. 48, No. 3, pp. 805-812, 2010.
[20] R. Tang, Y. Shi, Z. Hou, and L. Wei, "Carbon nanotube-based chemiresistive sensors", *Sensors*, Vol. 17, No. 4, pp. 882, 2017.
[21] J. H. Rouse, "Polymer-assisted dispersion of single-walled carbon nanotubes in alcohols and applicability toward carbon Nanotube/Sol-Gel composite formation", *Langmuir*, Vol. 21, No. 3, pp. 1055-1061, 2005.
[22] S. F. Liu, L. C. Moh, and T. M. Swager, "Single-walled carbon nanotube–metalloporphyrin chemiresistive gas sensor arrays for volatile organic compounds", *Chem. Mater.*, Vol. 27, No. 10, pp. 3560-3563, 2015.
[23] B. Yoon, S. J. Choi, T. M. Swager, and G. F. Walsh, "Switchable single-walled carbon nanotube–polymer composites for CO_2 sensing", *ACS Appl. Mater. Interfaces*, Vol. 10, No. 39, pp. 33373-33379, 2018.
[24] S. J. Choi, B. Yoon, S. B. Lin, and T. M. Swager, "Functional Single-Walled Carbon Nanotubes for Anion Sensing", *ACS Appl. Mater. Interfaces*, Vol. 12, No. 25, pp. 28375-28382, 2020.
[25] B. Yoon, and S. J. Choi, "Selective acetate recognition and sensing using SWCNTs functionalized with croconamides", *Sens. Actuator B-Chem.*, Vol. 346, No. 130461, pp. 1-8, 2021.